

# In situ measurements of Krypton in Xenon gas with a quadrupole mass spectrometer following a cold-trap at a temporarily reduced pumping speed

---

**Ethan Brown\***, Stephan Rosendahl, Christian Huhmann, Christian Weinheimer,  
**Hans Kettling**

*Institut für Kernphysik, University of Münster, Wilhelm-Klemm-Str. 9, D-48149 Münster,  
Germany  
Email: ethanbrown@uni-muenster.de*

**ABSTRACT:** A new method for measuring trace amounts of krypton in xenon using a cold trap with a residual gas analyzer has been developed, which achieves an increased sensitivity by temporarily reducing the pumping speed while expending a minimal amount of xenon. By partially closing a custom built butterfly valve between the measurement chamber and the turbomolecular pump, a sensitivity of 40 ppt has been reached. This method has been tested on an ultra-pure gas sample from Air Liquide with an unknown intrinsic krypton concentration, yielding a krypton concentration of  $330 \pm 200$  ppt.

**KEYWORDS:** Xenon; Krypton; Mass spectrometry; Cold trap.

---

\*Corresponding author.

---

## Contents

<b>1. Introduction</b>	<b>1</b>
<b>2. Enhanced Gas Content Measurements using a Residual Gas Analyzer with a Liquid Nitrogen Cold Trap</b>	<b>2</b>
<b>3. Experimental Setup</b>	<b>3</b>
<b>4. Measurements</b>	<b>9</b>
<b>5. Analysis</b>	<b>11</b>
<b>6. Conclusion</b>	<b>12</b>
<b>7. Acknowledgement</b>	<b>14</b>

---

## 1. Introduction

Xenon detectors are used for a large number of low background particle physics experiments, including direct dark matter detection, neutrinoless double beta decay, and solar neutrino searches [1] - [3]. Such experiments, which look for extremely rare interactions, require an ultra low intrinsic background. Xenon detectors are currently among the most sensitive detectors for these type of experiments, and have pushed the technological and scientific limits in various fields [4] [5] for several reasons. Due to the high  $Z$  value, xenon detectors shield external gamma backgrounds at the central region of the detector. Xenon also has a low intrinsic radioactivity, as it has no long lived radioactive isotopes, except for  $^{136}\text{Xe}$  [5] [6], which is the subject of double beta decay searches, and hence has a low enough rate to be ignored as a background in other experiments at current sensitivities. Additionally, xenon detectors can be scaled to large volumes with relative ease, allowing for incredible sensitivity for these rare event searches on a short time scale.

However, to achieve a sufficiently low background for these rare event searches, at the level of  $10^{-2}$  dru<sup>1</sup>, internal impurities must be reduced substantially relative to what is available in commercial xenon. One such impurity that has an important impact on xenon detectors is  $^{85}\text{Kr}$ , which has a beta decay with an endpoint energy of 687 keV.  $^{85}\text{Kr}$  is created in nuclear fuel reprocessing and was formerly created in nuclear weapons testing, but with a relatively long half life of 10.8 years, both sources contribute to the present concentration in the atmosphere at a level of  $10^{-11}$   $^{85}\text{Kr}$  in Kr.  $^{85}\text{Kr}$  must be removed from commercial xenon to achieve the low internal background

---

<sup>1</sup>differential rate unit: 1 dru = 1 event / keV / kg / day

necessary for modern astroparticle physics experiments. Commercially available xenon can be purchased with an intrinsic contamination of less than 10 ppb<sup>2</sup> Kr in Xe, but the low background requirements dictate that this fraction must be further reduced to levels below 1 ppt<sup>3</sup>.

<sup>85</sup>Kr is commonly removed from xenon by reducing the total amount of Kr in the gas via cryogenic distillation [7]. It is of key importance to be able to measure the amount of krypton in xenon, both for the input gas at the level of 10 ppb, as well as down to the best purity levels currently achievable at the sub-ppt level. While several methods exist to make this measurement, we present here a method that can be performed with common equipment used in gas laboratories with nearly zero xenon consumption. Moreover, this is a fast, online method that can be performed in situ, as opposed to offline methods that require up to weeks to obtain a result.

## 2. Enhanced Gas Content Measurements using a Residual Gas Analyzer with a Liquid Nitrogen Cold Trap

Mass spectrometry devices are capable of measuring the mass composition of gas samples, but due to the limitations of the dynamic range of such devices, they cannot be used in standard operation to measure trace impurity concentrations at the ppt level. One technique to enhance the sensitivity of this measurement is to use a liquid nitrogen cold trap to reduce concentration of the dominant gas species by orders of magnitude, thereby allowing a quantitative measurement of the trace impurities without saturating the mass spectrometer. This method has already been developed to measure various impurities in xenon gas [8] - [10], and has been investigated further for the particular case of measuring the concentration of krypton in xenon at the sub ppt level [11].

The principle behind the sensitivity enhancement of this measurement lies in the difference of vapor pressures of xenon and the impurities of interest at 77 K, in this case krypton. At this temperature, xenon has a vapor pressure of  $2.5 \times 10^{-3}$  mbar, while that of krypton is orders of magnitude higher at 2.0 mbar [12], as shown in figure 1. Independent of the incoming flow rate, the cold trap reduces the xenon pressure to the vapor pressure, allowing the krypton to pass through more or less unattached<sup>4</sup>. This allows enough krypton to be introduced to the mass spectrometer to measure the trace concentration while maintaining the low pressure necessary to operate the device.

In this work, modifications are introduced that address two important issues. First, the amount of gas used for the measurement is drastically reduced, allowing for many measurements without expending large amounts of xenon. This is of key importance for applying this method for long-term quality assurance purposes on large quantities of xenon, since xenon is quite expensive. This is realized by reducing the flow rate of xenon into the system and also by making measurements on

---

<sup>2</sup>1 ppb =  $10^{-9}$  mol/mol

<sup>3</sup>1 ppt =  $10^{-12}$  mol/mol

<sup>4</sup>The concept of vapor pressure describes the equilibrium between the gaseous phase of an atom or molecule with the solid or liquid phase. It is governed by the atom-atom or molecule-molecule binding energies in the liquid or solid phase but it neglects surface-atom or surface-molecule binding effects, which depend very much on the surfaces of the recipient. Only if one or more monolayers of the atom or molecule is covering the walls the atom-atom or molecule-molecule interaction takes over and vapor pressure is a good concept. Therefore, we expect deviations from this simple concept of the vapor pressure at low amounts of atoms or molecules.

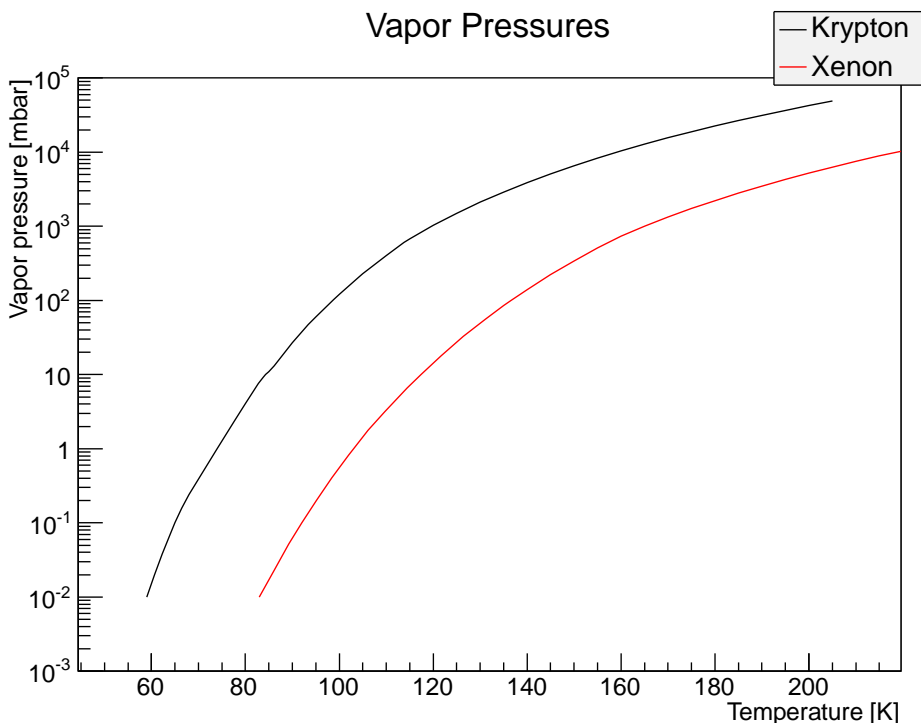


**Figure 1.** Vapor pressures of xenon and krypton [12]. While no data are available for xenon at 77 K, extrapolation of the xenon curve yields a value of  $2.5 \times 10^{-3}$  mbar, which is consistent with the 3 order of magnitude difference between xenon and krypton at slightly higher temperatures.

a relatively short time scale. Using this approach it is possible to measure the krypton concentration in a very nearly non-destructive way.

The second issue addressed here is an additional sensitivity enhancement by temporarily reducing the pumping speed in the measurement chamber. Mass spectrometry devices must typically be operated at a pressure below  $10^{-5}$  mbar, and are therefore usually installed very near a turbomolecular pump (TMP), ensuring that the vacuum stays well below the required limit. By partially closing a valve in front of the turbo pump for a short time, the pressure rises, thus enhancing the sensitivity to all gas species. In order to maintain safe operation of the mass spectrometer, the scan range is set only to the trace masses of interest, so that the increased pressure of the bulk gas components does not saturate the device.

Finally, in order to make quantitative analyses of the Kr/Xe fraction in gas samples in the ppb range and below, a calibration method has been developed where krypton can be artificially doped in a xenon sample over a large range of concentrations. To achieve this, a volume division method has been established, which allows doping at the ppb level and facilitates a quantitative measurement of krypton in xenon to levels below 1 ppb.

### 3. Experimental Setup

A diagram of the experimental apparatus used for our measurements is shown in figure 2. The gas sample is introduced by opening valve V1, after which the gas passes a low conductance differential

pumping section before entering a liquid nitrogen cold trap. There is an additional low conductance differential pumping section between the cold trap and the main chamber where the measurement is performed. The main chamber houses a Transceptor II quadrupole mass spectrometer [13]. A custom made butterfly valve is mounted between the main chamber and the TMP used to evacuate the system.

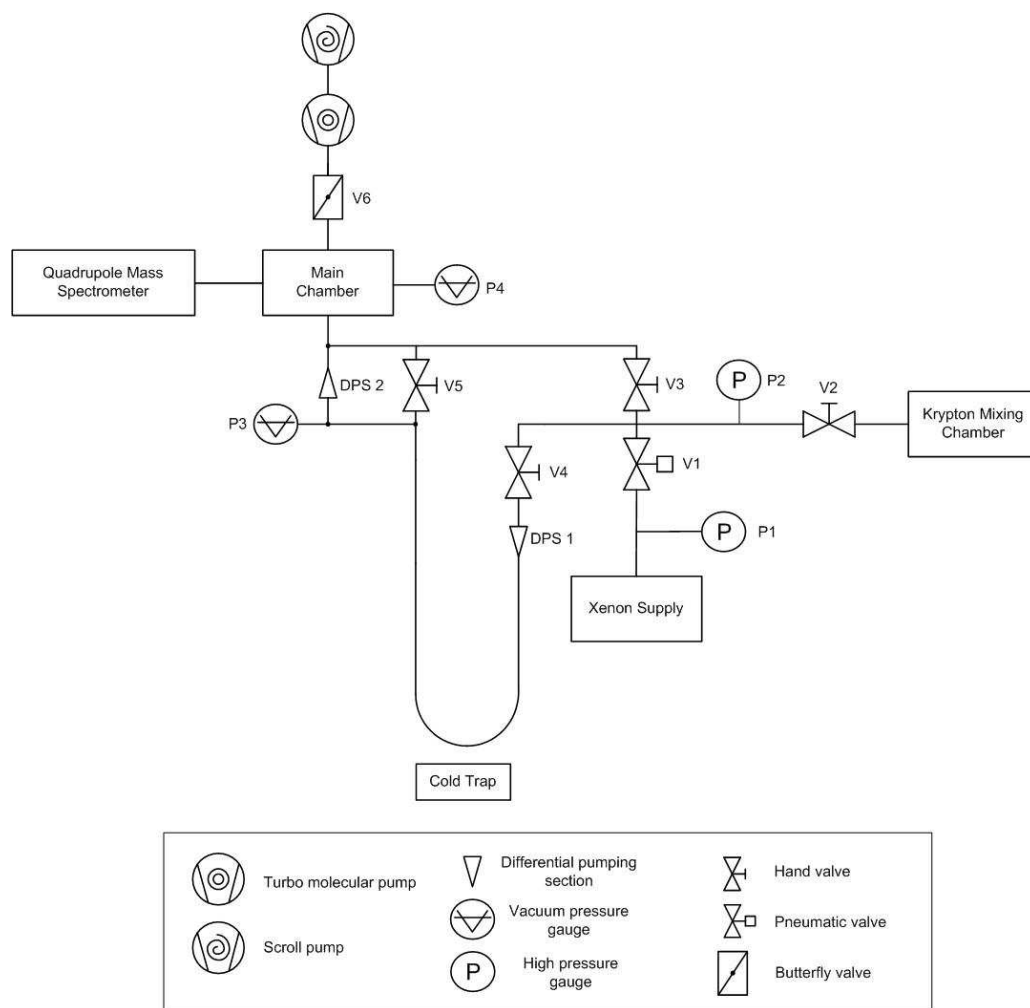


**Figure 2.** Diagram of experimental setup.

The key difference between our setup and that described in reference [8] is the presence of the custom made butterfly valve located between the main chamber and the TMP, which allows to reproducibly reduce the pumping speed, thereby enhancing the sensitivity to trace gases. As shown in figure 3, the butterfly valve consists of a cylindrical plate 1 mm thick with a 54.6 mm diameter mounted on a rotational feedthrough. The plate can be turned to partially block the opening in the CF100 flange in which it is mounted, whose inner diameter is 55 mm. The position of the butterfly valve can be controlled with better than 1° precision.

In order to optimize the sensitivity enhancement, the mass spectrometer can be operated only in the mass range of the trace gas of interest. In the case of krypton in xenon, where the dominant



**Figure 3.** Custom built butterfly valve, which partially closes the opening between the main chamber and the TMP, reducing the effective pumping speed. The position of the valve is controlled by a rotational feedthrough.

gas component is xenon, limiting the range from 76 to 90 atomic mass units (amu) allows operation of the mass spectrometer at pressures above the specification of  $10^{-5}$  mbar with a high sensitivity to krypton without damaging the ion detection electronics since the partial pressure remains sufficiently low.

An understanding of the gas flow through the system is outlined here by treating only the xenon flow through the system. While there is a mass dependence of the gas flow, an understanding of the xenon flow through the system is sufficient to conduct the measurements. The different behavior of krypton gas in the system is accounted for by using calibrations with krypton gas at many different concentrations. This allows the behavior of krypton relative to xenon to be absorbed into the fit parameters introduced in the analysis.

The gas flow through the system is naturally divided into two sections at the cold trap, since most of the gas freezes at this point. Before the cold trap, the flow dynamics are dominated by the limited conductivity through the first differential pumping section DPS1 while after the cold trap the conductivity of the second differential pumping section and butterfly valve are most important.

In the region before the cold trap, the flow can be measured simply by the time rate of change of the inlet pressure  $p_{in}$ . For a fixed volume of gas  $V$ , the flow  $q_{in}$  is given by,

$$q_{in} = -V \frac{dp_{in}}{dt}. \quad (3.1)$$

Figure 4 shows the flow rate of a sample measurement. Additionally, the flow is related to the conductivity of the differential pumping section  $C_1$  by,

$$q_{in} = C_1 \Delta p \approx C_1 p_{in}, \quad (3.2)$$

since the pressure after the leak valve is much smaller than  $p_{in}$ . Alternatively, the conductivity can be calculated in the laminar flow regime by,

$$C_1 = \frac{\pi d^4}{256 \eta l} p_{in}, \quad (3.3)$$

where  $d = 0.13$  mm is the inner diameter and  $l = 100$  mm is the length of the differential pumping section, and  $\eta = 2.3 \times 10^{-5}$  Pa s is the viscosity of xenon at 293 K. The conductivity of DPS1 is shown in figure 5 as measured by equation (3.2). At low inlet pressures, a linear behavior of the conductivity is observed, typical of laminar flow. While the precise value of the conductivity is not of crucial importance, a conductivity in this range is necessary to optimize the sensitivity to krypton and the consumption of xenon.

The Reynolds number, which is used to determine when a flow becomes turbulent, is given by

$$Re = \frac{4\rho q}{\pi\eta p_{in}d}, \quad (3.4)$$

where  $q$  is the flow rate. A Reynolds number below 2500 indicates the flow is laminar, and a Reynolds number above 4000 indicates it is turbulent, while intermediate values correspond to a transitional regime. At low inlet pressures around  $p_{in} = 100$  mbar, the Reynolds number is  $Re = 250$ , consistent with laminar flow. At  $p_{in} = 300$  mbar, where the conductivity begins to show non-linearity, the Reynolds number is  $Re = 3000$ . At a higher inlet pressure of  $p_{in} = 600$  mbar, a value of  $Re = 7900$  is consistent with turbulent flow.

### Input flow evolution

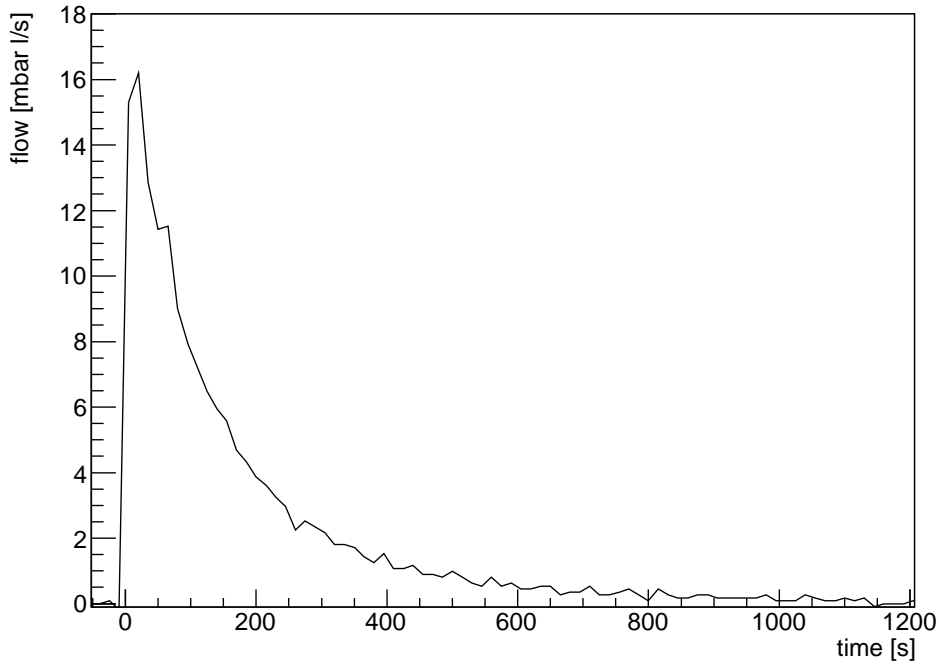


**Figure 4.** Flow evolution at the gas inlet for an example measurement as measured by the time rate of change of the inlet pressure.

## Conductivity of DPS1

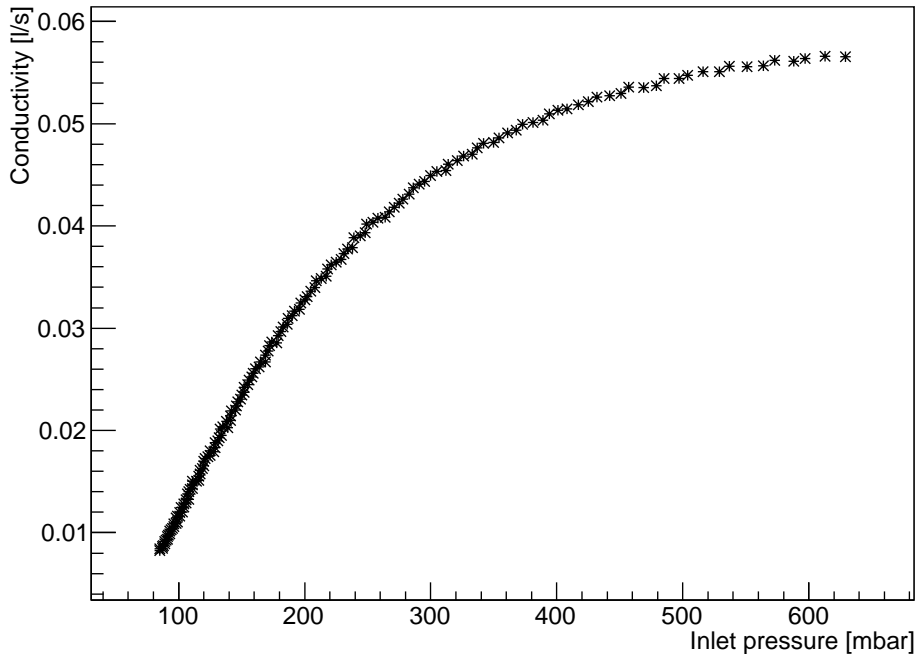


**Figure 5.** Conductivity  $C_1$  of DPS1 as a function of inlet pressure as measured by equation (3.2). The linear dependence of the conductivity at low inlet pressure is typical of laminar non-turbulent flow. The non-linear behavior at higher pressure is due to the flow becoming turbulent.

At the cold trap, where the bulk of the gas freezes, the partial pressure of each gas does not exceed the vapor pressure at liquid nitrogen temperature. We consider here the cases of xenon and krypton.

Xenon has a vapor pressure of  $2.5 \times 10^{-3}$  mbar at 77 K while that of krypton is 2.6 mbar, which allows the krypton to pass through the cold trap unattached, since the partial pressure of krypton is always well below this value. As mentioned in footnote <sup>4</sup>, this is not fully true, since some krypton can attach to the wall of the cold trap by atom-surface interactions. Indeed, after warming up the cold trap, we see some krypton coming out of the trap. Even for a high krypton concentration, say from a doping measurement with 10000 ppb Kr/Xe, the krypton partial pressure in the inlet volume is around  $10^{-2}$  mbar, well below the vapor pressure. Since the pressure is substantially reduced between the inlet and the cold trap, the partial pressure of krypton in the cold trap is always substantially below this. In practice, the pressure in the cold trap is slightly higher than the xenon vapor pressure, and is measured to be  $2.5 \times 10^{-2}$  mbar, but since the pressure in the cold trap was monitored a full understanding of the gas dynamics is still possible. In principle, a cold trap with a larger surface area may fully freeze the xenon, but this pressure reduction was adequate to perform measurements.

The total gas pressure is then further reduced in the measurement chamber by the use of a second low conductance differential pumping section, DPS2. Since at these low pressures the gas flow is in the molecular flow regime, it is possible to calculate the conductivity  $C_2$  through DPS2,



which is given by

$$C_2 = \frac{\pi}{16} \cdot \bar{c} \cdot d^2 \frac{14 + 4\frac{l}{d}}{14 + 18\frac{l}{d} + 3(\frac{l}{d})^2} \quad (3.5)$$

where  $l = 5$  mm is the length of the tube and  $d = 1$  mm is the diameter, and

$$\bar{c} = \sqrt{\frac{8RT}{\pi M}} \quad (3.6)$$

is the mean particle speed. We use a value of  $\bar{c} = 217$  m/s for xenon at  $T = 293$  K, which corresponds to a conductivity of  $C_2 = 8 \times 10^{-3}$  l/s.

Note that even with the use of the cold trap and the much higher vapor pressure of krypton relative to xenon, the dominant component of the gas is still xenon. This is due to the fact that the krypton concentration is so low.

The xenon ice in the cold trap provides a constant pressure source of gas to the differential pumping section, which enters the main chamber and is pumped away by the TMP. The flow into the main chamber  $q_{MC}$  is given by equation (3.2), with  $C_1$  replaced by  $C_2$  and  $p_{in}$  replaced by the pressure in the cold trap  $p_{CT} = 2.5 \times 10^{-2}$  mbar, yielding a flow of  $q_{MC} = 2 \times 10^{-4}$  mbar l/s.

The flow out of the main chamber  $q_{out}$  is determined by the pressure in the main chamber  $p_{MC}$  and the effective pumping speed of the TMP  $S_{eff}$ ,

$$q_{out} = p_{MC} \cdot S_{eff}, \quad (3.7)$$

The effective pumping speed is reduced from the full pumping speed  $S$  due to the presence of the butterfly valve between the TMP and the main chamber, which has a conductivity  $C_B$ , and is related by,

$$\frac{1}{S_{eff}} = \frac{1}{C_B} + \frac{1}{S}. \quad (3.8)$$

An estimation of conductivity of the butterfly valve in the fully open position can be found by treating it as a simple aperture, and is given by

$$C_B = \frac{\pi d^2}{16} \bar{c}, \quad (3.9)$$

where  $d$  is the diameter of the aperture and  $\bar{c}$  is the mean particle speed given in equation (3.6). The aperture of the butterfly valve has a diameter of  $d = 55$  mm, which corresponds to a conductivity of  $C_B = 130$  l/s. With a pumping speed of  $S = 300$  l/s, this corresponds to an effective pumping speed of  $S_{eff} = 90$  l/s. The pressure in the main chamber during a measurement with the butterfly valve fully open is around  $p_{MC} = 1.5 \times 10^{-6}$  mbar, yielding a flow out of the chamber of  $q_{out} = 1.4 \times 10^{-5}$  mbar l/s, in fair agreement with the flow into the chamber.

The final dynamical consideration of the system is the gas flow out of the turbo pump when the butterfly valve is partially closed. With the butterfly valve set to  $14^\circ$  from fully closed, the setting used for the measurements, the pressure in the main chamber was  $p_{MC} = 5 \times 10^{-5}$  mbar. With this, the effective pumping speed for xenon is reduced by a factor of 30, to  $\tilde{S}_{eff} = 3$  l/s.

Calibrations were performed using xenon samples artificially doped with krypton. The doping proceeded by use of volume division. A sample of krypton was placed in a small volume at 1.0

bar, and then expanded into a second volume which was larger by a factor of 5.6. The large volume was then evacuated with a TMP and the process was repeated. The pressure in the small volume was monitored with a Baratron MKS type 121A pressure sensor, which is accurate to 0.5% in the range of 1 mbar to 10 bar. The pressure sensor eliminates the need for a precise calibration of the volume sizes, but such a calibration was performed as a cross check and was found to be consistent. Finally, the krypton at a reduced pressure is mixed with xenon in an equally sized volume at 2 bar to allow for a precise doping to levels of  $10^{-3}$ . To achieve doping levels at lower concentrations, the volume division process can be repeated on a gas sample at a doping level around  $10^{-3}$ , to reach lower doping concentrations.

#### 4. Measurements

To perform a measurement, a gas sample with known doping is prepared. The cold trap is prepared with the liquid nitrogen filled to roughly the same level around the trap for 10 minutes before beginning the measurement. Repeated measurements show that the precise level of the nitrogen is not important. The RGA is set to scan only the trace krypton isotopes, a range from 76 to 90 amu, which avoids potential saturation effects in the RGA at xenon mass units.

The gas sample is prepared and its pressure is monitored by the pressure sensor P2. Just before beginning a measurement, the pumping speed of the TMP is reduced by partially closing the butterfly valve to  $14^\circ$  from fully closed. The gas sample is then introduced into the system by opening valve V4, and the mass spectrum is recorded in the pre-defined range. The gas is fed into the system for several minutes, and the hand valve V4 is then closed. The pressure in the main chamber is always monitored to ensure that the total pressure stays in a safe range for operation of the RGA.

The RGA records the current at steps of 0.2 amu. The current for a given mass number is found by integrating over three steps with 0.2 amu difference centered around the mass of interest. This was chosen to optimize the signal to noise ratio.

An example measurement is shown in figure 6. In this case, a gas sample with a krypton doping of 53000 ppb was used. The gas sample is introduced at  $t = 200$  s, and the krypton signal appears in the RGA after a short delay. This delay is dependent on the krypton concentration and is longer at lower concentrations. The delay is likely due to surface effects, where a finite amount of krypton attaches to the surface of the cold trap before equilibrium is reached, but after this short time the remainder of the krypton passes through unattached<sup>4</sup>. The figure shows the time behavior of several krypton isotopes, which are treated in detail in section 5. The signal peaks shortly after the sample is introduced, then decreases as the input pressure drops, and hence the flow rate is reduced.

Since the input pressure and gas flow are not constant over the measurement, a correction must be made in order to perform a proper quantitative analysis of the krypton concentration. The current is normalized by the input flow between  $t = 400$  s and  $t = 550$  s by applying a correction

$$I_c(t) = I(t) \times \frac{q(t)}{q_0}, \quad (4.1)$$

where  $q_0 = 10$  mbar l/s is used as a reference flow rate. The resulting flow corrected current is shown in figure 7. The corrected current is nearly flat after normalization, thus confirming that

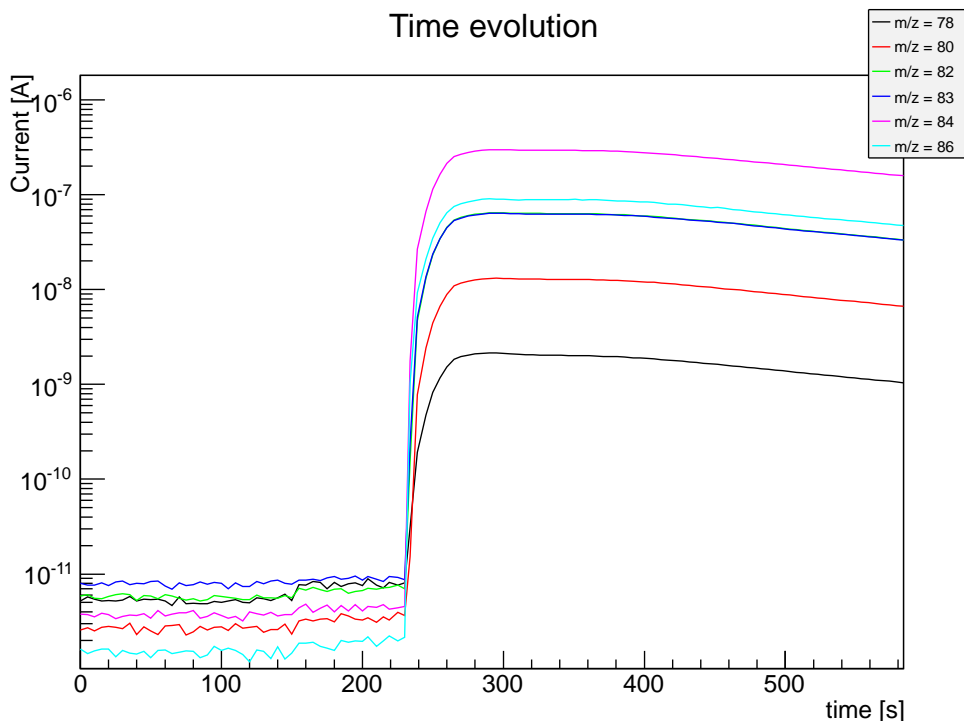


**Figure 6.** Example measurement showing the time evolution of krypton isotopes

this yields the correct time-dependent correction. For analyzing the measurements, this region is averaged.

One important aspect of this measurement technique is that it consumes only a small amount of xenon. Since xenon is expensive, it is useful to be able to perform a quantitative gas analysis repeatedly without expending a large amount of gas.

For calibration measurements with high doping concentrations and for undoped measurements, the amount of xenon gas required is minimal. Only that necessary to fill the inlet volume plus feed lines to a supply bottle is required. In practice, volumes much smaller than one liter can easily be constructed. In our setup, the total volume was around 30 ml, and xenon gas was introduced at 2 bar. While some gas remained in the inlet volume after the measurement, it was discarded for practical reasons. Thus, each measurement expended 0.06 standard liters of xenon, but this can likely be reduced for future measurements by designing a system where one does not need to exhaust the remaining sample gas after the measurement and possibly by recovering the xenon frozen in the cold trap. For comparison, the method presented by Dobi et al [11] consumes around 8 standard liters per measurement. Thus, our measurement method is essentially non-consuming compared to other similar measurement methods.

For the low concentration doping calibration measurements, more xenon was necessary due to the extra step of mixing the dilute krypton with xenon in the dilution procedure. Here, the inlet volume must be filled as many as three times, yielding a total of 0.18 standard liters for the measurement. However, these calibration measurements do not necessarily need to be repeated for measuring multiple gas samples, so this is not a routine requirement for gas consumption.

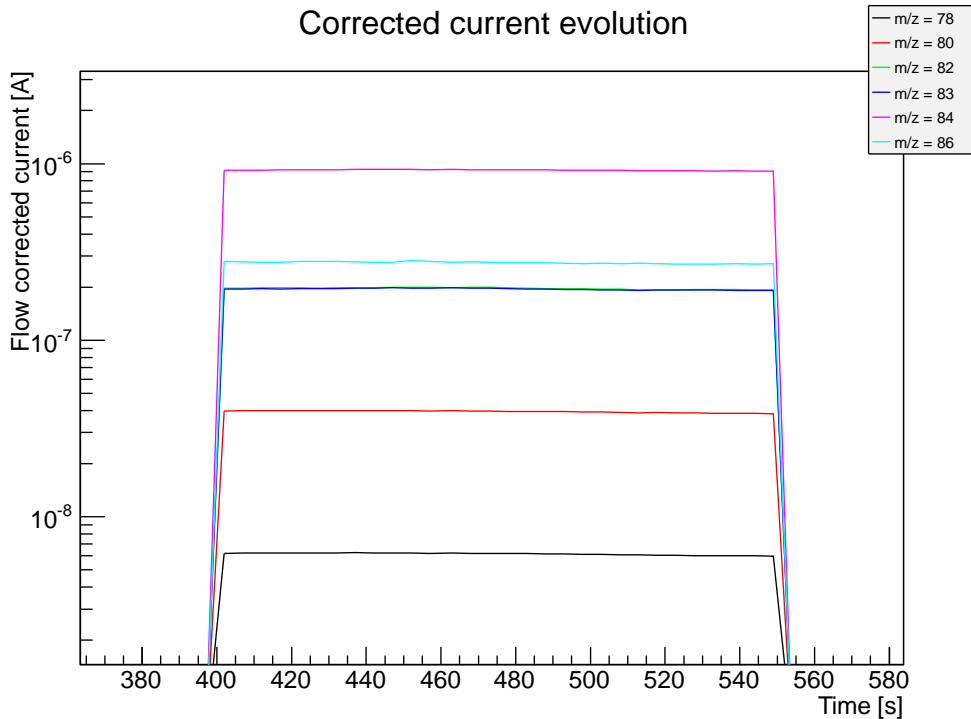


**Figure 7.** Example measurement with normalization by flow rate. Note that the relative currents for the different isotopes follow the expectations presented in table 1 below.

## 5. Analysis

Several measurements were made with a sample of xenon purchased from Air Liquide. This high purity gas is specified to have a Kr/Xe concentration below 10 ppb, but the absolute concentration is not measured by the company. We use these measurements to several ends, as an illustration of this procedure for measuring trace amounts of krypton in xenon, to infer the ultimate sensitivity of the measurement, and also to determine the actual Kr/Xe concentration of the Air Liquide gas. This last point is important for the context of using cryogenic distillation to further reduce the krypton contamination, since the input concentration is of some importance.

In order to determine the unknown concentration in the xenon, several measurements were made with the RGA cold trap setup with known dopings at 61,000 ppb, 53,000 ppb, 28,000 ppb, 830 ppb, 700 ppb, 25 ppb, 10 ppb and 9 ppb, as well as two undoped samples.

Within one measurement, additional information can be obtained by treating each isotope separately, since different isotopes are present at different concentrations for the same doping. The krypton isotopes considered in this analysis and their relative natural abundances are listed in table 1. The factor of nearly 160 between the abundance of  $^{84}\text{Kr}$  and that of  $^{78}\text{Kr}$  allows the study of the response of the measurement procedure to a large range of concentrations with a single measurement.

To find the relationship between the corrected current  $I$  and the concentration  $c$ , all data points with and without doping that were clearly above the background were fit with a linear function of

Isotope	Abundance $f$
$^{78}\text{Kr}$	0.35%
$^{80}\text{Kr}$	2.25%
$^{82}\text{Kr}$	11.6%
$^{83}\text{Kr}$	11.5%
$^{84}\text{Kr}$	57.0%
$^{86}\text{Kr}$	17.3%

**Table 1.** Krypton isotopes and their relative natural abundance [12].

the form,

$$I(c) = a \times f \times c = a \times f \times (d + c_0), \quad (5.1)$$

where  $c = d + c_0$  is the total concentration,  $d$  is the doping concentration,  $c_0$  is the intrinsic concentration, and  $f$  is the isotopic fraction. The free fit parameters are the normalization constant  $a$  and the intrinsic concentration  $c_0$ .

Figure 8 shows the data as well as linear fits to all data and subsets thereof using equation 5.1. Of key interest is the fact that each measurement shows a linear behavior, while there is a rather large discrepancy between different measurements. The data also lie in two distributions, one for the high dopings and another for lower dopings. This is likely due to a systematic effect that is yet to be fully understood, but to show a demonstration of the measurement method this is simply accounted for in a systematic error, which is then the dominant error on the measurement process.

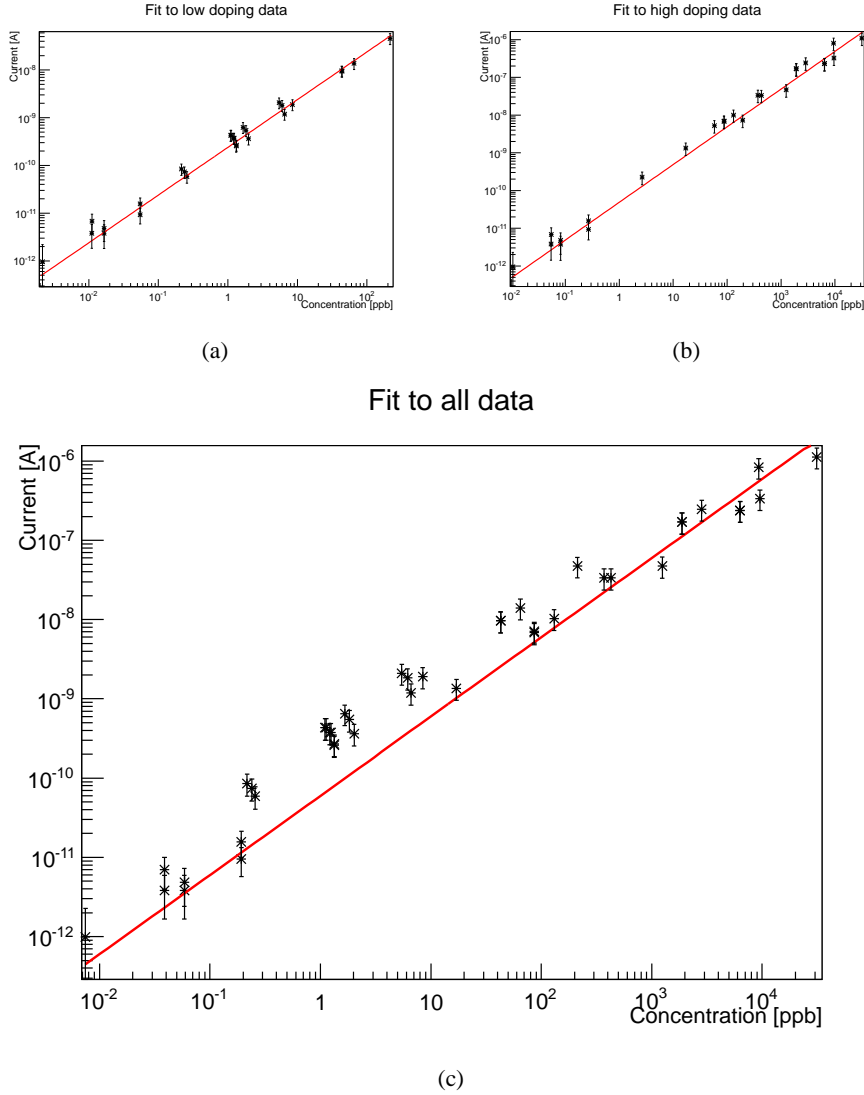
Figure 8(a) and 8(b) show the fits to the low and high doping data separately. The error is treated as two terms, a constant error due to electronic noise and background in the RGA, and a relative error due to effects that impact the concentration in the measurement chamber. The constant error,  $\Delta I_0 = 2.0 \times 10^{-12}$  A comes from the variation of the slope of the undoped data sets, where two measurements with identical dopings were possible. The relative error,  $\frac{\Delta I}{I} = 0.30$  comes from the variation in the slopes of the doped data sets. This combination of errors yields a reduced  $\chi^2$  of 0.96 and 1.04 for the low and high doping fits respectively.

Figure 8(c) shows the fit to all data, using the same error treatment as in the fits to the subsets, giving a reduced  $\chi^2$  of 1.6. The fits to the different subsets of data yield concentrations of 470 ppt, 420 ppt, and 100 ppt, from which we claim a value on the intrinsic concentration of  $c_0 = 330 \pm 200$  ppt.

Finally, to estimate the sensitivity of this measurement method, we exploit the spread in the isotopic abundance in the undoped measurements. The isotopes with the lowest abundance are not clearly visible above the background, but the isotopes whose current is larger than the background can be used to determine the sensitivity. Since mass 80 is measured at the level of the background, but not clearly above it, our sensitivity for detection is likely above this level. We thus use masses 82 and 83, whose abundances are 11.6% and 11.5% respectively, which yield a sensitivity of 40 ppt.

## 6. Conclusion

A new method for measuring trace impurities in xenon gas has been described, where concentra-



**Figure 8.** Data from doped and undoped measurements with a linear fit with equation 5.1. Figure 8(a) shows only the low doping data, yielding fit parameters of  $a = (240 \pm 10) \times 10^{-12}$  A/ppb and  $c_0 = 0.10 \pm 0.02$  ppb. Figure 8(b) shows only the high doping data, which gives fit parameters of  $a = (49 \pm 4) \times 10^{-12}$  A/ppb and  $c_0 = 0.50 \pm 0.02$  ppb. Figure 8(c) shows all data, with fit parameters of  $a = (59 \pm 3) \times 10^{-12}$  A/ppb and  $c_0 = 0.34 \pm 0.21$  ppb. The dominant error on  $c_0$  comes from fitting to the different subsets of data.

tions of krypton in xenon down to the sub ppb level can be detected. The key features of this measurement method are the sensitivity increase obtained by temporarily reducing the pumping speed at the measurement chamber by partially closing a custom-made butterfly valve and the minimal amount of xenon necessary for the measurement. Using this method, the krypton concentration in a sample of xenon from Air Liquide was measured at  $330 \pm 200$  ppt, and the sensitivity of this measurement was estimated at 40 ppt. An independent measurement of the krypton concentration in the same Air Liquide gas was performed by our colleagues from the Max Planck Institute for Nuclear Physics in Heidelberg using gas chromatography yielding an intrinsic concentration of  $370 \pm 80$  ppt [14]. This independent check matches our result well, thus confirming our result. By

further reducing the systematic uncertainties, we might be able to achieve uncertainties close to the sensitivity limit for future measurements.

Our measurement method will be used for several applications. First, it can be used as a screening device for cryogenic distillation. It can be used to measure the input krypton concentration, which is expected to be in the ppb range. It can also be used to measure the krypton enriched xenon that comes from the high concentration end of the distillation column, allowing for an estimate of the purity of the clean gas by comparison with the incoming gas. Finally, it can be used as a leak detector for ultra pure gas at the sub ppt level. An air leak would result in a large increase in the krypton concentration, which would be detectable with the cold trap enhanced RGA measurement. Thus one can monitor the stability of an ultra clean system with a minimum expenditure of gas.

In addition to measuring krypton concentrations, this setup can measure any impurity whose boiling point is below that of nitrogen. Although these measurements have not yet been explored in detail, future work will address quantitative analyses of such impurities.

## 7. Acknowledgement

This work was supported by Deutsche Forschungsgemeinschaft. We thank Alexander Fieguth, Michael Murra, and Martin Schlak for help with construction and measurements.

## References

- [1] A. Aprile et al., *The XENON100 dark matter experiment*, *Astropart. Phys.* 35 (2012), 573 - 590.
- [2] M. Auger et al., *The EXO-200 detector, part I: detector design and construction*, 2012 *JINST* 7 P05010.
- [3] A. Aprile et al., *Liquid xenon detectors for particle physics and astrophysics*, *Rev. Mod. Phys.* 82, 2053 - 2097 (2010).
- [4] A. Aprile et al., *Dark Matter Results from 225 Live Days of XENON100 Data*, *Phys. Rev. Lett.* 109, 181301 (2012).
- [5] N. Ackerman et al. (EXO Collaboration), *Observation of a two-neutrino double-beta decay in  $^{136}\text{Xe}$  with the EXO-200 detector*, *Phys. Rev. Lett.* 107 (2011).
- [6] A. Gando et al., *Measurement of the double- $\beta$  decay half-life of  $^{136}\text{Xe}$  with the KamLAND-Zen experiment* *Phys. Rev. C* 86 021601 (2012).
- [7] K. Abe et al., *Distillation of liquid xenon to remove krypton*, *Astroparticle Physics*, 31(4):290 - 296, (2009).
- [8] D.S. Leonard et al., *A simple high-sensitivity technique for purity analysis of xenon gas*, *Nuclear Instruments and Methods in Physics Research Section A: Accelerators, Spectrometers, Detectors and Associated Equipment*, 621:678 - 684, 2010.
- [9] A. Dobi et al., *A xenon gas purity monitor for EXO*, *Nuclear Instruments and Methods in Physics Research Section A: Accelerators, Spectrometers, Detectors and Associated Equipment* (September 2011).

- [10] A. Dobi et al., *Xenon purity analysis for EXO-200 via mass spectrometry*, Nuclear Instruments and Methods in Physics Research Section A: Accelerators, Spectrometers, Detectors and Associated Equipment, 675(0):40 - 46, 2012.
- [11] A. Dobi et al., *Detection of krypton in xenon for dark matter applications*, Nuclear Instruments and Methods in Physics Research Section A: Accelerators, Spectrometers, Detectors and Associated Equipment, 665(0):1 - 6, (2011).
- [12] D. R. Lide, *CRC Handbook of Chemistry and Physics*, 87th edition, 2006-2007, CRC Press
- [13] INFICON Holding AG, Hintergase 15B, CH-7310 Bad Ragaz, Switzerland.
- [14] Sebastian Lindemann, Max Planck Institute for Nuclear Physics, Heidelberg, Private communication.